Commun Nonlinear Sci Numer Simulat 43 (2017) 158–170

Contents lists available at ScienceDirect

Commun Nonlinear Sci Numer Simulat

journal homepage: www.elsevier.com/locate/cnsns

Research paper

Geometry and dynamics of fast magnetosonic wavefronts near magnetic null points

Manuel Núñez*

Depto. Análisis Matemático, Universidad de Valladolid, 47011 Valladolid, Spain

ARTICLE INFO

Article history:
Received 17 February 2016
Revised 29 June 2016
Accepted 1 July 2016
Available online 1 July 2016

PACS:
42.15.Dp
47.40.Nm
52.35.Bj
94.20.Wf

Keywords:
Fast magnetosonic waves
Magnetic null points
Geometrical optics
Shock formation

ABSTRACT

The behavior of two-dimensional fast magnetosonic waves in the vicinity of isolated points where the magnetic field vanishes is studied analytically. The geometry of rays and wavefronts is described, and the curvature of both is found using conformal mapping techniques. These results are applied to the formation of shock waves, obtaining that shock formation is guaranteed at a finite time for any initial condition of the perturbation when the wavefront is concave and the rays tend to focus, whereas otherwise shocks occur only for a certain range of initial conditions.

1. Introduction

Magnetohydrodynamic waves play a major role in many astrophysical phenomena, notably in the processes of magnetic reconnection and generation of solar flares as occur in the solar corona. Among the vast observational literature we will only mention [1]. Since magnetic nulls play an important role in the classical theory of fast magnetic reconnection, a theoretical study of MHD waves in their vicinity seemed worth pursuing. Some of the former papers consider waves depending only on the distance to a simple null point [2,3]; more realistic geometries followed. In [4] it is shown how fast magnetosonic waves in a nonhomogeneous coronal plasma refract in regions of low Alfvén velocity. In a series of papers [5–7] McLaughlin, Hood and their collaborators studied the shape of MHD waves as they approach the null point. Generation of shocks, magnetic reconnection and formation of solar flares near null points are analyzed e.g. in [8,9]. In several (but not all) of these papers, it is assumed that the plasma has a low beta, which means that the kinetic pressure gradient vanishes from the momentum equation. Independently of the physical justification of this hypothesis as concerns coronal plasma, it is theoretically logical: without a variable pressure the fast magnetosonic wave travels at the Alfvén speed $c_A = B/\sqrt{\rho}$, the Alfvén wave at $|\mathbf{B}\cdot\mathbf{n}|/\sqrt{\rho}$, and the slow wave does not move at all. Thus magnetic null points, where the Alfvén velocity vanishes, act as a breaker against any MHD wave, which cannot surpass it. By contrast, a positive sound speed would allow the waves to cross

* Fax: +34-983423013.
E-mail address: mnjmhd@am.uva.es

http://dx.doi.org/10.1016/j.cnsns.2016.07.001
1007-5704/

the null, albeit more slowly. The naive intuition that zero-β MHD waves impacting a null point would curl around it turns out to be roughly accurate.

The mathematical treatment of the problem usually starts from the ideal (non diffusive) MHD system and study numerically the evolution of MHD waves with a variety of initial and boundary conditions. While this procedure is probably the only possible one as soon as the background magnetic field presents a minimum of complexity, it is always desirable to have a fully analytic study as long as the simplicity of the magnetic geometry allows it. Accordingly we have considered the geometry of rays and wavefronts of the fast magnetosonic wave near a X-point in dimension two; to start from a static equilibrium we need the field to be current free, i.e. irrotational. In a neighborhood of the null, rays behave as logarithmic spirals; that is, their trajectory is given by

$$t \to \exp(-At)(\cos(Bt), \sin(Bt)),$$

for some $A > 0$. The shape of wavefronts is more complex as it depends on the initial condition, but a neat trick with conformal mappings enable us the see these wavefronts as the image of a family of curves transported by a family of straight lines. This fact will enable to find the curvature of both rays and wavefronts, which will be crucial in the final section, where we consider the formation of magnetosonic shocks. The key tool is an equation satisfied by the jump of the time differential of the solutions of a quasilinear hyperbolic system propagating into an equilibrium state. This has been used for some time for the purely hydrodynamic case [10,11], as well as for the magnetohydrodynamic one [12], and in full generality [13,14]. It turns out that this quantity satisfies a transport equation along the rays which has the form of a Riccati differential equation, whose solutions may tend to infinity in a finite time; this is taken as the signal of the formation of a shock wave. This is related to the blow-up of a perturbation wave of low amplitude and high frequency, as presented in [15,16] in the context of weakly nonlinear geometrical optics. In the last case the Riccati equation is substituted by a partial differential one of Burgers' type, but the time of blow-up is similar in both approaches, which also fail after formation of caustics. We will apply these techniques to see if fast waves approaching the magnetic null form shocks; much depends on the form of the wavefront, with concave ones focusing rays and creating blow-ups.

2. Geometry of rays and wavefronts

The fast magnetosonic wavefronts in a medium with zero velocity are the surfaces $\tau = \text{const.}$, where τ satisfies the following particular case of the eikonal equation:

$$\frac{\partial \tau}{\partial t} = \pm c_A |\nabla \tau|, \tag{1}$$

where $c_A = B/\sqrt{\rho}$ is the Alfvén velocity, $\mathbf{B}$ the magnetic field and ρ the density (see e.g.[17]). Solution of (1) depends on the initial condition $\tau(0)$, and is not guaranteed to exist for all time. Let $\mathbf{n}$ be the normal vector

$$\mathbf{n} = \frac{\nabla \tau}{|\nabla \tau|}. \tag{2}$$

If we want the waves to propagate in the direction of $\mathbf{n}$ we must take the minus sign in (1). The equations satisfied by the rays $t \to \mathbf{x}(t)$ may be set in a variety of modes (see e.g. [14,16]), but since c_A does not depend on $\mathbf{n}$, they may be simplified to

$$\begin{aligned} \frac{d\mathbf{x}}{dt} &= c_A \mathbf{n} \\ \frac{d\mathbf{n}}{dt} &= \mathbf{n} \cdot (\mathbf{n} \cdot \nabla c_A) - \nabla c_A. \end{aligned} \tag{3}$$

In this case rays are orthogonal to wavefronts. The basic state is a static plane equilibrium with constant pressure (low beta approximation), which means that the magnetic field must be current free, i.e. irrotational. In this case the field is the gradient of a harmonic function. We assume that this function has a simple zero at $\mathbf{x} = \mathbf{0}$. Higher order zeroes are unlikely to occur, since they are intrinsically unstable; if x_0 is an isolated zero of higher order of a function f, $f(x_0) = 0$, a small perturbation of f may split the zero in several simple ones or it may vanish altogether: think of $f(x) = x^2$, $x_0 = 0$. Thus, by making a linear change of variables we may represent the field as

$$\mathbf{B}(x, y) = (y, x) + O(x^2 + y^2), \tag{4}$$

We assume that the density is smooth and does not vanish at $\mathbf{0}$,

$$\rho = \rho_0 + O(\sqrt{x^2 + y^2}), \tag{5}$$

Let $a = 1/\sqrt{\rho_0}$. In polar coordinates, c_A may be written as

$$c_A = ar + O(r^2). \tag{6}$$

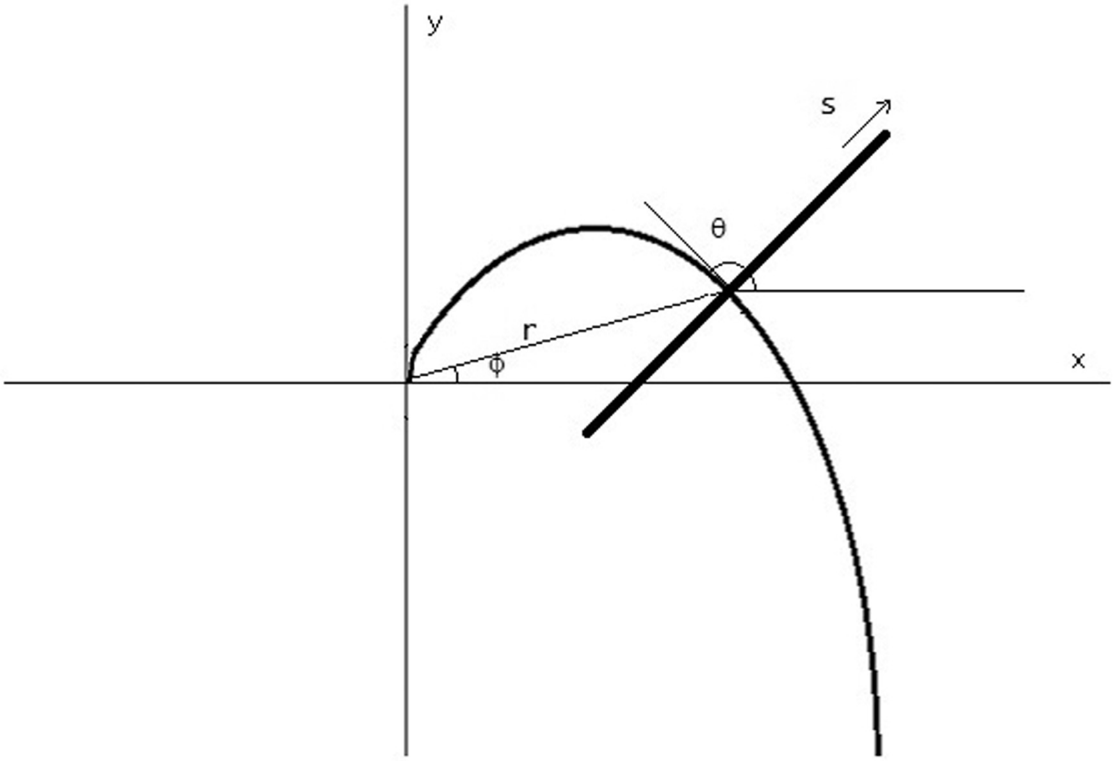

Fig. 1. The main parameters.

Since $\mathbf{n}$ is unitary, it may be written as $\mathbf{n} = (\cos\theta, \sin\theta)$. Then (3) translates as

$$\begin{aligned} \dot{x} &= c_A \cos\theta \\ \dot{y} &= c_A \sin\theta \\ \dot{\theta} &= (\sin\theta)\frac{\partial c_A}{\partial x} - (\cos\theta)\frac{\partial c_A}{\partial y}. \end{aligned} \tag{7}$$

The dot denotes time derivatives. Switching to polar coordinates $x = r\cos\phi$, $y = r\sin\phi$, and denoting $' = d/dr$, (7) becomes

$$\begin{aligned} \dot{r} &= c_A \cos(\theta - \phi) \\ \dot{\phi} &= \frac{c_A}{r}\sin(\theta - \phi) \\ \dot{\theta} &= c_A' \sin(\theta - \phi) + O(r). \end{aligned} \tag{8}$$

Let $\alpha = \theta - \phi$, $\beta = \theta + \phi$. α and β are derived quantities and therefore not important as variables. The rest of them are illustrated in Fig. 1, where the curve ending at the origin is the ray (later shown to be a logarithmic spiral) and the thick orthogonal one is the wavefront (later to be parameterized by s). We may write (8) as

$$\begin{aligned} \dot{r} &= c_A \cos\alpha \\ \dot{\alpha} &= \left(c_A' - \frac{c_A}{r}\right)\sin\alpha + O(r) \\ \dot{\beta} &= \left(c_A' + \frac{c_A}{r}\right)\sin\alpha + O(r). \end{aligned} \tag{9}$$

Omitting the remainder, the second equation admits a first integral

$$\frac{d}{dt}(\ln|\tan(\alpha/2)|) = c_A' - \frac{c_A}{r}. \tag{10}$$

Making the derivative of the first equation of (9) with respect to t,

$$\begin{aligned} \ddot{r} &= c_A'\dot{r}\cos\alpha - c_A(\sin\alpha)\dot{\alpha} + O(r) \\ &= \left(2\frac{c_A'}{c_A} - \frac{1}{r} + O(1)\right)(\dot{r})^2 - c_A c_A' + \frac{c_A^2}{r} + O(r^2). \end{aligned} \tag{11}$$

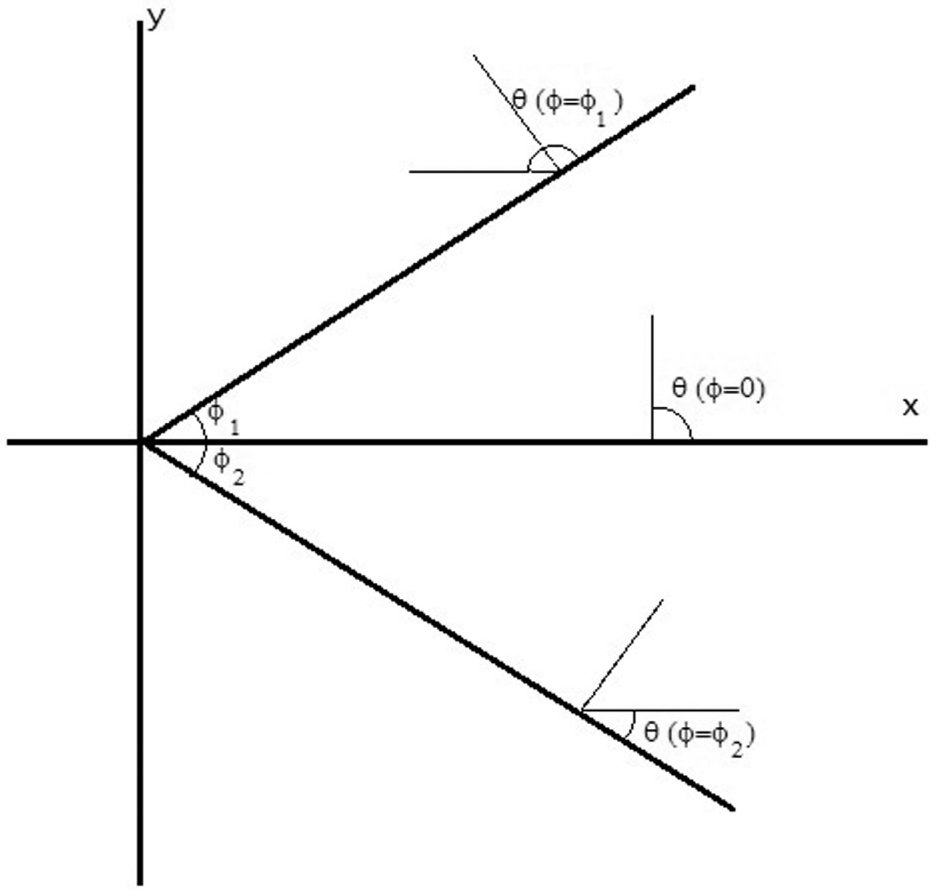

Fig. 2. Minimum original angles.

By introducing the expression in (6), (11) becomes

$$\ddot{r} = \left(\frac{1}{r} + O(1)\right)(\dot{r})^2 + O(r^2). \tag{12}$$

Recovering a more standard notation for clarity,

$$\frac{d}{dt}\left(\frac{1}{r}\frac{dr}{dt}\right) = \frac{1}{r}\left(\frac{dr}{dt}\right)^2 O(1) + O(r) = O(r). \tag{13}$$

Thus to the first order in r,

$$r(t) = r(0)\exp(kt), \tag{14}$$

with

$$k = \frac{\dot{r}(0)}{r(0)} = a\cos(\theta(0) - \phi(0)) + O(r). \tag{15}$$

This is the equation of a logarithmic spiral. If c_A is precisely ar, the ray would spiral outwards for $\cos(\theta(0) - \phi(0)) > 0$, inwards for $\cos(\theta(0) - \phi(0)) < 0$, and describe circumferences if this quantity equals zero. In general, the first order approximation is only valid for rays approaching the magnetic null, i.e. we must assume that the original angles satisfy $\cos(\theta(0) - \phi(0)) < 0$. The valid θ's are therefore those greater than the angle drawn in the example of Fig. 2 for three different choosing of ϕ; notice that these must be larger as ϕ grows, as expected from following logarithmic spirals. Taking this result to (10), we obtain that to the first order the expression in the left hand side is constant along the ray, so that α is also constant, i.e.

$$\alpha = \alpha(0) + O(r) = \theta(0) - \phi(0) + O(r). \tag{16}$$

As for β, (9) becomes

$$\dot{\beta} = (2a + O(r))\sin\alpha = (2a + O(r))(\sin\alpha(0) + O(r)). \tag{17}$$

Hence, to the first order,

$$\beta(t) = \beta(0) + 2at\sin\alpha(0). \tag{18}$$

Recovering θ and ϕ from α and β, we find to the first order

$$\begin{aligned}\theta(t) &= \theta(0) + at\sin\alpha(0)\\ \phi(t) &= \phi(0) + at\sin\alpha(0).\end{aligned} \tag{19}$$

Hence near the point $\mathbf{0}$, the ray has approximately the equation

$$t \to r(0)\exp(at\cos\alpha(0))(\cos(\phi(0) + at\sin\alpha(0)), \sin(\phi(0) + at\sin\alpha(0))). \tag{20}$$

Writing the equation in complex form, the ray is the image by the exponential mapping of the straight line

$$t \to \ln r(0) + i\phi(0) + at(\cos\alpha(0) + i\sin\alpha(0)). \tag{21}$$

This will be useful in elucidating the geometry of the wavefronts. Recall that a point does not determine the ray passing through it; a normal vector to the wavefront at this point must also be provided. The correct course is to start from a given wavefront and see how it evolves at least in the vicinity of the magnetic null point. Say this wavefront is given by a curve $s \to \mathbf{g}(s)$. For each point of it, we have its argument $\phi(s)$ as well as the argument $\theta(s)$ of the normal vector to the curve at this point; obviously this angle must be chosen consistently, as we will precise later. The rays starting at the points of the curve with the direction of the normal tend to the magnetic null if the condition

$$\cos\alpha(s) = \cos(\theta(s) - \phi(s)) < 0, \tag{22}$$

holds. The successive wavefronts are then the orthonormal curves to the family of rays indexed by s. Orthonormal curves are notoriously unreliable, tending to cut themselves for all but the most regular configurations. This is precisely what happens with wavefronts, and description of the wave dynamics complicates considerably after formation of caustics. To avoid this as far as possible we will consider a short wavefront, say formed by $\mathbf{g}(s)$ for $s \in (s_0 - \delta, s_0 + \delta)$.

Rays are therefore given by a modified (20):

$$t \to r(s)\exp(at\cos\alpha(s))(\cos(\phi(s) + at\sin\alpha(s)), \sin(\phi(s) + at\sin\alpha(s))). \tag{23}$$

To find the orthogonal curves looks forbidding, but since the complex exponential is a conformal mapping, these curves are the image of the orthogonal curves to the family of straight lines

$$t \to \ln r(s) + i\phi(s) + at(\cos\alpha(s) + i\sin\alpha(s)). \tag{24}$$

These are much easier to analyze. If the curve $\mathbf{g}$ is convex in the direction of the normal vector, the lines will diverge and wavefronts will not cut; if concave, they will form caustics, but up to this point we may study the dynamics equally well. Each of the lines given by (24) has the equation

$$\begin{aligned} t &\to \mathbf{g}(s) + at\mathbf{m}(s)\\ |\mathbf{m}| &= 1, \quad \mathbf{m}\cdot\mathbf{g}' = 0.\end{aligned} \tag{25}$$

Thus the orthogonal lines will be curves of the form

$$t \to \mathbf{g}(s) + at(s)\mathbf{m}(s). \tag{26}$$

The orthogonality condition is

$$(\mathbf{g}'(s) + at'(s)\mathbf{m}(s) + at(s)\mathbf{m}'(s))\cdot\mathbf{m}(s) = 0. \tag{27}$$

Since $\mathbf{m}\cdot\mathbf{m}' = \mathbf{m}\cdot\mathbf{g}' = 0$, this means $t'(s) = 0$, so that t is constant; that is, orthogonal curves are formed from the original one $\mathbf{g}$ by transport along the lines at constant velocity. As we see in (24), in our case this velocity is a,

$$\begin{aligned}\mathbf{g}(s) &= (\ln r(s), \phi(s))\\ \mathbf{m}(s) &= (\cos\alpha(s), \sin\alpha(s)).\end{aligned} \tag{28}$$

Thus the wavefronts are the images of these curves for fixed t, i.e. they have the form

$$s \to r(s)\exp(at\cos\alpha(s))(\cos(\phi(s) + at\sin\alpha(s)), \sin(\phi(s) + at\sin\alpha(s))). \tag{29}$$

Given the arbitrariness of the functions of s within (30), the curvature of wavefronts seems impossible to find. However, its asymptotic value for large t may be found. Recall that for any plane curve (x, y), the signed curvature is given by

$$\kappa = \frac{x'y'' - x''y'}{(x'^2 + y'^2)^{3/2}}. \tag{30}$$

Writing this curve with the complex numbers notation, $g = x + iy$, and denoting by - the complex conjugate $\overline{g} = x - iy$, (30) may be written as

$$\kappa = \frac{\mathrm{Im}(\overline{g'}g'')}{|g'|^3}, \tag{31}$$

where $'$ denotes differentiation with respect to the parameter of the curve. Assume that U is an open set in the complex plane $\mathbb{C}$ such that $g(s) \in U$ for all s, and let $f : U \to \mathbb{C}$ be an analytic function. It is well known that

$$\begin{aligned}(f\circ g)' &= (f'\circ g)g' \\ (f\circ g)'' &= (f''\circ g)(g')^2 + (f'\circ g)g'',\end{aligned} \tag{32}$$

where f', f'' denotes the first and second derivatives of f as an analytic function. Applying (31) to the curve $f\circ g$, we obtain

$$\kappa_{f\circ g} = \frac{\mathrm{Im}(\overline{f'(g)}f''(g)|g'|^2 g' + |f'(g)|^2\overline{g'}g'')}{|f'(g)g'|^3}. \tag{33}$$

Consider the case $f(z) = \exp(z)$, so that $f = f' = f''$. Then $|f(z)| = \exp(\mathrm{Re}z)$, and therefore

$$\kappa_{f\circ g} = \exp(-\mathrm{Re}g)\left[\frac{\mathrm{Im}g'}{|g'|} + \frac{\mathrm{Im}(\overline{g'}g'')}{|g'|^3}\right] = \exp(-\mathrm{Re}g)\left[\frac{\mathrm{Im}g'}{|g'|} + \kappa_g\right]. \tag{34}$$

When applying this formula to a straight line such as the ones given by (21), $\kappa_g = 0$, and

$$\kappa_{f\circ g} = r(s)^{-1}\exp(-at\cos\alpha(s))\sin\alpha(s). \tag{35}$$

Notice that since $\cos\alpha(s) < 0$, this curvature tends exponentially to infinity. As stated, curvature of logarithmic spirals is simple anyway. The real usefulness of (34) comes from applying it to the wavefronts. We have seen (26) that the curves whose image are the wavefronts have the form

$$\mathbf{h} : s \to \mathbf{g}(s) + at\mathbf{m}(s). \tag{36}$$

To simplify the calculations assume that $\mathbf{g}(s) = (\xi(s), \eta(s))$ is parametrized by the arc length. Then $\mathbf{m}(s) = (-\eta'(s), \xi'(s))$,

$$h(t,s) = (\xi(s) - at\eta'(s)) + i(\eta(s) + at\xi'(s)). \tag{37}$$

Writing $\mathbf{m}(s) = (\cos\psi(s), \sin\psi(s))$, so that $\kappa = \psi'$, it es easy to check the following identities:

$$\begin{aligned}\kappa &= \xi'\eta'' - \xi''\eta' \\ \kappa^2 &= \xi''^2 + \eta''^2 \\ 0 &= \xi'\xi'' + \xi''^2 + \eta'\eta'' + \eta''^2 \\ \kappa^3 &= \xi''\eta''' - \xi'''\eta''.\end{aligned} \tag{38}$$

Applying (30) to (37), the curvature of the curve translated from the original one after at time t is

$$\kappa(t) = \frac{(\xi' - at\eta'')(\eta'' + at\xi''') - (\xi'' - at\eta''')(\eta' + at\xi'')}{[(\xi' - at\eta'')^2 + (\eta' + at\xi'')^2]^{3/2}}. \tag{39}$$

Using (38), we find

$$\kappa(t,s) = \frac{\kappa(0,s)}{|1 - at\kappa(0,s)|}. \tag{40}$$

This formula makes good sense: for curves convex in the sense of the normal, $\kappa(0, s) < 0$, the straight lines spread out and the transported curve tends to straighten, the curvature decreasing as $1/t$. If the curve is concave in the sense of the normal, $\kappa(0, s) > 0$ and the curvature blows up at $t = (a\kappa(0,s))^{-1}$, which is where nearby rays collide. Applying (34) to the real wavefront $f\circ g$, whose parameter is now s, we find

$$\kappa_{f\circ g}(t,s) = r(s)^{-1}\exp(-at\cos\alpha(s))\left[\frac{\mathrm{Im}\,\partial g/\partial s}{|\partial g/\partial s|} + \kappa(t,s)\right]. \tag{41}$$

$\kappa(t, s)$ is given by (40) and

$$\begin{aligned}\mathrm{Im}\,\partial g/\partial s &= \phi'(s) + at(\cos\alpha(s))\alpha'(s) \\ |\partial g/\partial s|^2 &= [(\ln r)'(s)]^2 + \phi'(s)^2 \\ &\quad + 2at\alpha'(s)[-(\ln r)'(s)\sin\alpha(s) + \phi'(s)\cos\alpha(s)] + a^2t^2\alpha'(s)^2.\end{aligned} \tag{42}$$

For t large,

$$\frac{\mathrm{Im}\,\partial g/\partial s}{|\partial g/\partial s|} \sim \frac{\alpha'(s)}{|\alpha'(s)|}\cos\alpha(s). \tag{43}$$

The direction of parametrization of $s \to g(t, s)$ is a matter of convention, but afterwards we will require that the tangent vector to the rays and the tangent vector to the wavefront form a positively oriented orthogonal pair in this order. Given the form in (26) and (28), this requires $\alpha'(s) > 0$. Hence, for t large,

$$\kappa_{f\circ g}(t,s) \sim r(s)^{-1}\exp(-at\cos\alpha(s))\left[\cos\alpha(s) + \frac{\kappa(0,s)}{|1 - at\kappa(0,s)|}\right], \tag{44}$$

for as long as the last term within the bracket does not blow up.

3. Formation of shock waves

3.1. General results

The rules of propagation of nonlinear waves in a static solution of a quasilinear hyperbolic system are well known [11,13,14]. Let us remember as briefly as possibly the main facts. Let

$$\frac{\partial \mathbf{u}}{\partial t} + \sum_j A_j(t, \mathbf{x}, \mathbf{u}) \frac{\partial \mathbf{u}}{\partial x_j} = \mathbf{0}, \tag{45}$$

be a quasilinear hyperbolic system, where all functions are assumed smooth enough. Let $\mathbf{u}_0$ be a known static solution of the system (45). Take a solution $\tau(t, \mathbf{x})$ of the eikonal equation

$$\det\left(\sum_j A_j(t, \mathbf{x}, \mathbf{u}_0) \frac{\partial \tau}{\partial x_j} + \frac{\partial \tau}{\partial t} I\right) = 0. \tag{46}$$

Assume that $\partial\tau/\partial t$ is an eigenvalue of order one of the matrix

$$A_\tau = \sum_j A_j(t, \mathbf{x}, \mathbf{u}_0) \frac{\partial \tau}{\partial x_j}, \tag{47}$$

and let $\mathbf{R}$ be a right eigenvector of A_τ, $\mathbf{L}$ a left eigenvector. In our case, the system will be the two-dimensional MHD one with zero beta, which is not strictly hyperbolic, but the results will hold as a limit case. Let $\Omega(t) : \tau(t, \mathbf{x}) = \text{const.}$, be a level surface of τ (a wavefront) separating two states, one of which is precisely $\mathbf{u}_0$. Eq. (46) corresponds to the characteristic surfaces of the system. Assume that the variable solution propagates into the state $\mathbf{u} = \mathbf{u}_0$, where the normal vector to Ω points. This means that

$$\frac{\partial \tau}{\partial t} < 0, \quad \mathbf{n} = \frac{\nabla\tau}{|\nabla\tau|}, \tag{48}$$

and the velocity of Ω is

$$c = -\frac{\partial\tau/\partial t}{|\nabla\tau|}. \tag{49}$$

We assume that $\mathbf{u}$ is continuous at both sides of Ω, but its derivatives may not be. Let $[\quad]$ denote the jump at Ω, i.e. the magnitude at the positive side of Ω, $\mathbf{u} = \mathbf{u}_0$, minus the one on the negative side. Then it may be shown that

$$\left[\frac{\partial \mathbf{u}}{\partial t}\right] = w_0 \mathbf{R}, \tag{50}$$

for a scalar $w_0(t, \mathbf{x})$ whose evolution along the rays will be studied. For any matrix $A(t, \mathbf{x}, \mathbf{u})$ we use the following notation:

$$(\nabla_u A) \cdot \mathbf{R} = \sum_i R_i \frac{\partial A}{\partial u_i}, \tag{51}$$

all of them evaluated at $\mathbf{u}_0$. Let

$$q_0 = \mathbf{L} \cdot \left(\sum_j \frac{n_j}{c} (\nabla_u A_j) \cdot \mathbf{R}\right) \cdot \mathbf{R}. \tag{52}$$

Notice that in the case of the fast wave $c = c_A$. To define the coefficient p_0 we need a more complicated formula [14], but for the two-dimensional case we may simplify it somewhat. We start with an orthogonal network of rays and wavefronts, as described in the previous section. Let us consider a single ray, say $s = s_0$, and parametrize it by the arc length ξ. Since in our case the rays are normal to the wavefronts,

$$\mathbf{n} \cdot \nabla = \frac{\partial}{\partial \xi} = \frac{1}{c_A} \frac{\partial}{\partial t}. \tag{53}$$

Take for every point of the ray a tangent vector $\mathbf{T}$ to the wavefront such that $\{\mathbf{n}, \mathbf{T}\}$ form a positively oriented orthogonal pair, and denote

$$A_n = \sum_j n_j A_j, \quad A_T = \sum_j T_j A_j. \tag{54}$$

Parametrize each wavefront in a neighborhood of s_0 by the arc length σ. Now we define

$$\begin{aligned} p_0 =& \mathbf{L}\cdot\left[A_n(\mathbf{u}_0)\frac{\partial\mathbf{R}}{\partial\xi}+A_T(\mathbf{u}_0)\frac{\partial\mathbf{R}}{\partial\sigma}\right] \\ &+\mathbf{L}\cdot\left[(\mathbf{R}\cdot\nabla_u A_n(\mathbf{u}_0))\frac{\partial\mathbf{u}_0}{\partial\xi}+(\mathbf{R}\cdot\nabla_u A_T(\mathbf{u}_0))\frac{\partial\mathbf{u}_0}{\partial\sigma}\right]. \end{aligned} \tag{55}$$

Finally let $q = q_0(\mathbf{L}\cdot\mathbf{R})^{-1},\ p = p_0(\mathbf{L}\cdot\mathbf{R})^{-1}$. Let $t \to \mathbf{x}(t)$ represent a ray associated to the phase τ, $w(t) = w_0(t, \mathbf{x}(t))$. Then w satisfies

$$\frac{dw}{dt} + pw + qw^2 = 0. \tag{56}$$

This is a Riccati equation without an independent term, so it may be reduced to a linear one:

$$\frac{d}{dt}\left(\frac{1}{w}\right) - \frac{p}{w} - q = 0, \tag{57}$$

whose solution is

$$\frac{1}{w(t)} = \frac{1}{w(0)}\exp\left(\int_0^t p(s)\,ds\right) + \exp\left(\int_0^t p(s)\,ds\right)\int_0^t \exp\left(-\int_0^s p(r)\,dr\right)q(s)\,ds. \tag{58}$$

Hence, if there exists t_1 such that

$$\frac{1}{w(0)} = -\int_0^{t_1}\exp\left(-\int_0^s p(r)\,dr\right)q(s)\,ds, \tag{59}$$

then $w(t)$ tends to ∞ when $t \to t_1$, which means that the jump of the differential tends to infinity. Hence $\mathbf{u}$ undergoes a jump and becomes discontinuous, which means that a shock appears.

The two-dimensional MHD pressureless system may be written in terms of the five-dimensional vector (expressed as a row instead of a column for typographical convenience)

$$\mathbf{u} = (B_1, B_2, v_1, v_2, \rho), \tag{60}$$

where $\mathbf{B}$ represents the magnetic field, $\mathbf{v}$ the velocity and ρ the density (see e.g. [18]). The subsequent calculations are essentially performed in [19]; however, in this case it is more convenient to take instead of the coordinate axes the system formed by $\{\mathbf{n}, \mathbf{T}\}$, i.e. the basis of $\mathbb{R}^5$ given by the vectors

$$\begin{aligned} (\mathbf{n}; \mathbf{0}; 0) &= (n_1, n_2, 0, 0, 0) \\ (\mathbf{T}; \mathbf{0}; 0) &= (-n_2, n_1, 0, 0, 0) \\ (\mathbf{0}; \mathbf{n}; 0) &= (0, 0, n_1, n_2, 0) \\ (\mathbf{0}; \mathbf{T}; 0) &= (0, 0, -n_2, n_1, 0) \\ (\mathbf{0}; \mathbf{0}; 1) &= (0, 0, 0, 0, 1), \end{aligned} \tag{61}$$

one finds that the matrices A_n and A_T of (54) are given by

$$A_n = v_n I + \begin{bmatrix} 0 & 0 & 0 & 0 & 0 \\ 0 & 0 & B_T & -B_n & 0 \\ 0 & B_T/\rho & 0 & 0 & 0 \\ 0 & -B_n/\rho & 0 & 0 & 0 \\ 0 & 0 & \rho & 0 & 0 \end{bmatrix}, \tag{62}$$

and

$$A_T = v_T I + \begin{bmatrix} 0 & 0 & -B_T & B_n & 0 \\ 0 & 0 & 0 & 0 & 0 \\ -B_T/\rho & 0 & 0 & 0 & 0 \\ B_n/\rho & 0 & 0 & 0 & 0 \\ 0 & 0 & 0 & \rho & 0 \end{bmatrix}. \tag{63}$$

The right and left eigenvectors of A_n are determined up to a multiplicative constant. After some calculations, we take them as

$$\begin{aligned} \mathbf{R} &= (B^2\mathbf{T};\ c_A B_T \mathbf{n} - c_A B_n \mathbf{T};\ \rho) \\ \mathbf{L} &= (B^2\mathbf{T};\ \rho c_A B_T \mathbf{n} - \rho c_A B_n \mathbf{T};\ 0), \end{aligned} \tag{64}$$

i.e. in the basis given by (61)

$$\mathbf{R} = (0, B^2, c_A B_T, -c_A B_n, \rho) \tag{65}$$

$$\mathbf{L} = (0, B^2, \rho c_A B_T, -\rho c_A B_n, 0). \tag{66}$$

Thus

$$\mathbf{L} \cdot \mathbf{R} = 2B^4. \tag{67}$$

One finds

$$q_0 = \frac{1}{c_A}\mathbf{L} \cdot (\nabla_u A_n \cdot \mathbf{R}) \cdot \mathbf{R} = 3B^4 B_T, \quad q = (3/2)B_T. \tag{68}$$

Let us find now $\partial\mathbf{R}/\partial\xi$ and $\partial\mathbf{R}/\partial\sigma$. to this end, denote b y κ_r the curvature of the ray and by κ_w the one of the wavefront at each point of the ray. Then

$$\begin{aligned} \frac{\partial \mathbf{n}}{\partial \xi} &= \kappa_r \mathbf{T} \qquad \frac{\partial \mathbf{T}}{\partial \xi} = -\kappa_r \mathbf{n} \\ \frac{\partial \mathbf{n}}{\partial \sigma} &= -\kappa_w \mathbf{T} \qquad \frac{\partial \mathbf{T}}{\partial \sigma} = \kappa_w \mathbf{n}. \end{aligned} \tag{69}$$

Thus, in the basis given in (61),

$$\frac{\partial \mathbf{R}}{\partial \xi} = \left(-B^2\kappa_r, \frac{\partial B^2}{\partial \xi}, \frac{\partial (c_A B_T)}{\partial \xi} + c_A B_n \kappa_r, -\frac{\partial (c_A B_n)}{\partial \xi} + c_A B_T \kappa_r, \frac{\partial \rho}{\partial \xi} \right), \tag{70}$$

and

$$\frac{\partial \mathbf{R}}{\partial \sigma} = \left(B^2\kappa_w, \frac{\partial B^2}{\partial \sigma}, \frac{\partial (c_A B_T)}{\partial \sigma} - c_A B_n \kappa_w, -\frac{\partial (c_A B_n)}{\partial \sigma} - c_A B_T \kappa_w, \frac{\partial \rho}{\partial \sigma} \right). \tag{71}$$

Since

$$\mathbf{u}_0 = (B_T\mathbf{T} + B_n\mathbf{n}; \mathbf{0}; 0), \tag{72}$$

we have

$$\frac{\partial \mathbf{u}_0}{\partial \xi} = \left(\frac{\partial B_n}{\partial \xi} - B_T\kappa_r, \frac{\partial B_T}{\partial \xi} + B_n\kappa_r, 0, 0, \frac{\partial \rho}{\partial \xi} \right), \tag{73}$$

$$\frac{\partial \mathbf{u}_0}{\partial \sigma} = \left(\frac{\partial B_n}{\partial \sigma} + B_T\kappa_w, \frac{\partial B_T}{\partial \sigma} - B_n\kappa_w, 0, 0, \frac{\partial \rho}{\partial \sigma} \right). \tag{74}$$

Now, since

$$\begin{aligned} \mathbf{L} \cdot A_n &= (0, c_A B^2, B^2 B_T, -B^2 B_n, 0) \\ \mathbf{L} \cdot A_T &= (-c_A B^2, 0, 0, 0, 0), \end{aligned} \tag{75}$$

we obtain the first two terms in the expression of p_0,

$$\begin{aligned} \mathbf{L} \cdot A_n \cdot \frac{\partial \mathbf{R}}{\partial \xi} &= \frac{3}{4} c_A \frac{\partial B^4}{\partial \xi} - B^4 \frac{\partial c_A}{\partial \xi} \\ \mathbf{L} \cdot A_T \cdot \frac{\partial \mathbf{R}}{\partial \sigma} &= -c_A B^4 \kappa_w. \end{aligned} \tag{76}$$

On the other hand,

$$\begin{aligned} \mathbf{L} \cdot (\nabla_u A_n \cdot \mathbf{R}) &= c_A B_T \mathbf{L} + (0, 0, B^4, 0, 0) \\ \mathbf{L} \cdot (\nabla_u A_T \cdot \mathbf{R}) &= -c_A B_n \mathbf{L}, \end{aligned} \tag{77}$$

so that

$$\begin{aligned} \mathbf{L} \cdot (\nabla_u A_n \cdot \mathbf{R}) \cdot \frac{\partial \mathbf{u}_0}{\partial \xi} &= c_A B^2 B_T \left(\frac{\partial B_T}{\partial \xi} + B_n \kappa_r \right) \\ \mathbf{L} \cdot (\nabla_u A_T \cdot \mathbf{R}) \cdot \frac{\partial \mathbf{u}_0}{\partial \sigma} &= c_A B^2 B_n \left(-\frac{\partial B_T}{\partial \sigma} + B_n \kappa_w \right). \end{aligned} \tag{78}$$

Adding all terms together,

$$p_0 = \frac{3}{4} c_A \frac{\partial B^4}{\partial \xi} - B^4 \frac{\partial c_A}{\partial \xi} - c_A B^4 \kappa_w + c_A B^2 B_T \left(\frac{\partial B_T}{\partial \xi} + B_n \kappa_r \right) + c_A B^2 B_n \left(-\frac{\partial B_T}{\partial \sigma} + B_n \kappa_w \right), \tag{79}$$

To find p we must divide p_0 by $2B^4$. After some manipulation and changing $\partial/\partial\xi$ to $\partial/\partial t$ using (53), we find

$$p = \frac{\partial}{\partial t} \left(\frac{B^{3/2}}{c_A^{1/2}} \right) - c_A \left(1 - \frac{B_n^2}{2B^2} \right) \kappa_w + c_A \frac{B_T B_n}{2B^2} \kappa_r + \frac{1}{4B^2} \frac{\partial B_T^2}{\partial t} - \frac{c_A B_n}{2B^2} \frac{\partial B_T}{\partial \sigma}. \tag{80}$$

3.2. Dynamics near the magnetic null

Recall that near the magnetic null $\mathbf{0}$, the rays are given by (23). Therefore

$$\mathbf{n}(t, s) = (\cos(\phi(s) + \alpha(s) + at \sin \alpha(s)), \sin(\phi(s) + \alpha(s) + at \sin \alpha(s))), \tag{81}$$

$$\mathbf{T}(t, s) = (-\sin(\phi(s) + \alpha(s) + at \sin \alpha(s)), \cos(\phi(s) + \alpha(s) + at \sin \alpha(s))). \tag{82}$$

Since to first order $\mathbf{B}(x, y) = (y, x),\ \rho = 1/a^2$, at a neighborhood of $\mathbf{0}$,

$$\begin{aligned} \mathbf{B}(t, s) =& r(s) \exp(at \cos \alpha(s)) (\sin(\phi(s) + \alpha(s) + at \sin \alpha(s)), \\ & \cos(\phi(s) + \alpha(s) + at \sin \alpha(s))) \\ B_n(t, s) =& r(s) \exp(at \cos \alpha(s)) \sin(2\phi(s) + \alpha(s) + at \sin \alpha(s)) \\ B_T(t, s) =& r(s) \exp(at \cos \alpha(s)) \cos(2\phi(s) + \alpha(s) + at \sin \alpha(s)). \end{aligned} \tag{83}$$

Notice that since $\alpha = \theta - \phi$, $2\phi + \alpha = \theta + \phi$. Let us analyze how each of the terms in (80) contributes to the integrand in (59), i.e. to the term

$$\exp\left(-\int_0^t p(r)\, dr \right). \tag{84}$$

1. We have

$$-\frac{\partial}{\partial t} \ln \left(\frac{B^{3/2}}{c_A^{1/2}} \right) = -\frac{\partial}{\partial t} \ln(B a^{-1/2}) = -\frac{\partial}{\partial t} \ln \left(a^{-1/2} r(s) \exp(at \cos \alpha(s) \right). \tag{85}$$

Thus its integral between 0 and t is $\ln(\exp(-at \cos \alpha(s))$, and the exponential of this value has the form $\exp(-at \cos \alpha(s))$. Recall that $\cos \alpha(s) < 0$, so this term grows exponentially in time.

2. The following term is

$$\begin{aligned} & c_A(t, s) \left(1 - \frac{B_n(t, s)^2}{2B(t, s)^2} \right) \kappa_w(t, s) \\ &= ar(s) \exp(at \cos \alpha(s)) \left(1 - \frac{1}{2} \sin^2(2\phi(s) + \alpha(s) + 2at \sin \alpha(s)) \right) \kappa_w(t, s) \\ &= ar(s) \exp(at \cos \alpha(s)) \left(\frac{3}{4} + \frac{1}{4} \cos(4\phi(s) + 2\alpha(s) + 4at \sin \alpha(s)) \right) \kappa_w(t, s). \end{aligned} \tag{86}$$

The value of κ_w is given by (40,41), and for t large, by (44). If we assume $\kappa(0, s) \le 0$, the corresponding term decays as $1/t$ and for t large

$$\kappa_w(t, s) \sim r(s)^{-1} \exp(-at \cos \alpha(s)) \cos \alpha(s). \tag{87}$$

Therefore the contribution of the term in (86) to the integral of $-p$ has the form

$$\frac{3}{4} at \cos \alpha(s) + \frac{\cos \alpha(s)}{4 \sin \alpha(s)} [\sin(4\phi(s) + 2\alpha(s) + 16at \sin \alpha(s)) - \sin(4\phi(s) + 2\alpha(s))]. \tag{88}$$

The last term is periodic in t and therefore bounded, so that its exponential is bounded above and below by positive constants and will have no significance on the convergence of the integral in (59).

If $\kappa(0, s) > 0$ the curvature κ_w behaves as

$$\kappa_w(t, s) \sim \frac{1}{|t - t_0|}, \tag{89}$$

as t nears $t_0 = (a\kappa(0, s))^{-1}$. Hence the integral of minus the term in (86) becomes infinite as t approaches t_0, and the same occurs for its exponential. In this case there is a finite blow-up time for the integral in (59). We will analyze later the meaning of this.

3. Let us consider now

$$-c_A(t,s)\frac{B_T(t,s)B_n(t,s)}{2B(t,s)^2}\kappa_r(t,s)$$
$$= -ar(s)\exp(at\cos\alpha(s))\sin(4\phi(s)+2\alpha(s)+4at\sin\alpha(s))\kappa_r(t,s). \tag{90}$$

κ_r is given by (35). Thus the primitive of this term is

$$-\frac{1}{16}\sin(4\phi(s)+2\alpha(s)+4at\sin\alpha(s)), \tag{91}$$

whose exponential is again bounded above and below.

4. The next term is

$$-\frac{1}{4B^2}\frac{\partial B_T^2}{\partial t}. \tag{92}$$

We have

$$B_T^2 = r^2\exp(2at\cos\alpha)\cos^2(2\phi+\alpha+at\sin\alpha)$$
$$\frac{\partial B_T^2}{\partial t} = r^2(2a)\cos\alpha\exp(2at\cos\alpha)\cos^2(2\phi+\alpha+at\sin\alpha)$$
$$- r^2\exp(2at\cos\alpha)\sin(4\phi+2\alpha+2at\sin\alpha)a\sin\alpha$$
$$-\frac{1}{4B^2}\frac{\partial B_T^2}{\partial t} = -\frac{1}{2}a\cos\alpha\left(1+\frac{1}{2}\cos(4\phi+2\alpha+2at\sin\alpha)\right)$$
$$+\frac{a}{4}\sin\alpha\sin(4\phi+2\alpha+2at\sin\alpha)$$
$$= -\frac{a}{2}\cos\alpha-\frac{1}{4}\cos(4\phi+3\alpha+2at\sin\alpha). \tag{93}$$

The primitive of this term is

$$-\frac{a}{2}t\cos\alpha-\frac{1}{8a\sin\alpha}[\sin(4\phi+3\alpha+2at\sin\alpha)-\sin(4\phi+3\alpha)], \tag{94}$$

and the second term is again a periodic function whose exponential is bounded above and below.

5. The last term is

$$\frac{c_AB_n}{2B^2}\frac{\partial B_T}{\partial\sigma}. \tag{95}$$

In the first place

$$\frac{c_AB_n}{2B^2} = \frac{a}{2}\sin(2\phi+\alpha+2at\sin\alpha)$$
$$\frac{\partial B_T}{\partial\sigma} = \frac{\partial}{\partial\sigma}[r(\sigma)\exp(at\cos\alpha(\sigma))\cos(2\phi(\sigma)+\alpha(\sigma)+2at\sin\alpha(\sigma)]. \tag{96}$$

While the expression is complex, we notice that it represents a function at most linear in t multiplied by the negative exponential $\exp(at\cos\alpha(\sigma))$. Therefore this is a function with finite integral in $(0,\infty)$, so that again its exponential is bounded above and below for all time. Combining all the terms, we find that for $\kappa(0,s)\le 0$,

$$\exp\left(-\int_0^t p(r)\,dr\right) = \exp\left[(at\cos\alpha)\left(-1+\frac{3}{4}-\frac{1}{2}\right)\right]H(t)$$
$$= \exp\left[-\frac{3}{4}(at\cos\alpha)\right]H(t), \tag{97}$$

where H is a function bounded above and below by positive constants. Since $q=(3/2)B_T$, Eq. (59) may be written

$$\frac{1}{w(0)} = -\int_0^{t_1}\frac{3}{2}H(t)\exp\left(\frac{at}{4}\cos\alpha\right)\cos(2\phi+\alpha+at\sin\alpha)\,dt, \tag{98}$$

where H, α and ϕ are specified to the ray $s=s_0$. The important thing is that the exponent $a(\cos\alpha)/4$ is negative, and therefore this integral is bounded for all time. Since in this case the integral $I(t_1)$ in (98) is bounded for all time, if we denote by M a constant such that $|I(t)|\le M$ for all t, and if we have $|w(0)|<1/M$, (98) cannot hold for any t_1. This shows that for small enough initial conditions, there is no shock formation at this ray.

Things are different when the original wavefront is concave, $\kappa(0,s_0)>0$. Then the integral behaves near t_0 as

$$-\int_0^{t_0}\frac{3}{2}H(t)\exp\left(\frac{1}{|t-t_0|}\right)\cos(2\phi+\alpha+at\sin\alpha)\,dt. \tag{99}$$

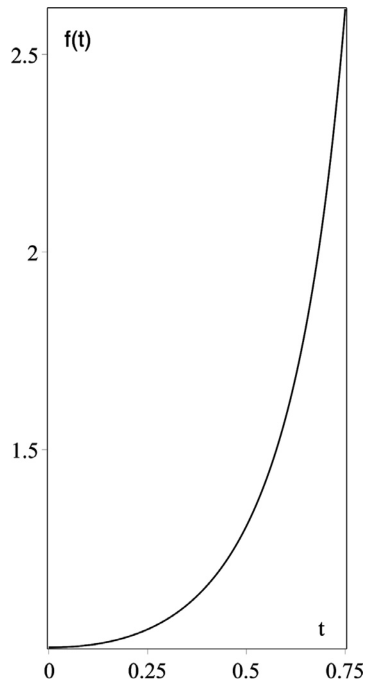

Fig. 3. Graph of the integrand function.

This value is infinite, even if $\cos(2\phi + \alpha + at_0 \sin\alpha) = 0$. This occurs because $\exp(1/|t - t_0|)$ grows so rapidly near t_0 that not even a factor of the form $t - t_0$ may tame it so that the integral is finite. We illustrate this by considering the graph of $f(t) = (1 - t)\exp(1/(1 - t))$ in Fig. 3; even drawing it in logarithmic scale, its extremely rapid growth is clear. Therefore the formation of a shock is guaranteed for any negative initial condition if the integral of (99) is infinite, for any positive initial condition if the integral is minus infinite. Which of the two things occurs depends on the sign of the cosine near t_0. Geometrically, when the wavefronts curl tightly near the magnetic null point, a shock is eventually formed.

4. Conclusions

There exists considerable theoretical and observational interest in the study of magnetohydrodynamic waves near magnetic null points. Even the simplest case of plane isolated magnetic nulls in zero beta plasmas has required so far numerical techniques to analyze the behavior of wavefronts at the vicinity of the critical point. The only clear fact is that waves do not surpass this point, which slows them down and acts as a breaker for all of them, but how they evolve near it or if they form shocks at a finite time presents considerable analytical difficulties. We concentrate on the fast magnetosonic wave and study its rays and wavefronts following geometrical optics techniques. When the original state represents a plane equilibrium and the zero of the magnetic field is of the first order, the ray equations may be approximately integrated near the zero and turn out to be logarithmic spirals. The shape and curvature of wavefronts depends in a complex way of the initial one, but the use of conformal mapping techniques allows us to find this curvature. This may go to infinite in a finite time if the original wavefront is concave or decay if it is convex, which makes good sense as in the first case rays tend to focus and caustics to appear. Once the geometry of rays and waves is established, we use the theory of solutions of hyperbolic systems propagating into static states to guess the possibility of formation of shocks in a finite time. The main equation is a Riccati one satisfied by the jump of the time derivative of a certain solution along a fixed ray; when the solution of this equation tends to infinity at a finite time, a shock occurs. After finding the coefficients of this equation, one finds that for concave wavefronts, a shock is certainly formed at a finite time for any initial condition; whereas for convex ones, only larger enough initial conditions will yield shocks. This last possibility may seem odd, as waves tend to crowd together near the magnetic null, which intuitively seems to point to shock creation. However, we must remember that waves travel at the Alfvén velocity and therefore slow near the critical point; this freezing may preclude blow ups at a finite time.

Acknowledgment

Partially supported by the Ministry of Economy and Innovation of Spain under contract MTM2012-31439.

References

[1] Nakariakov VM, Ofman L, Deluca EE, Roberts B, Davila JM. TRACE observation of damped coronal loop oscillations: implications for coronal heating. Science 1999;285:862–4.
[2] Bulanov SV, Syrovatskii SI. MHD oscillations and waves near a magnetic null line. Fiz Plazmy 1980;6:1205–18. Soviet J. of Plasma Phys., 6, 1980, 661–667
[3] Craig IJD, Watson PG. Fast dynamic reconnection at x-type neutral points. Astrophys J 1992;393:385–95.
[4] Nakariakov VM, Roberts B. On fast magnetosonic coronal pulsations. Sol Phys 1995;159:399–402.
[5] McLaughlin JA, Hood AW. MHD wave propagation in the neighborhood of a two-dimensional null point. Astron Astrophys 2004;420:1129–40.
[6] McLaughlin JA, Hood AW. Magnetohydrodynamics wave propagation in the neighborhood of two dipoles. Astron Astrophys 2006;452:603–13.
[7] McLaughlin JA, De Moortel I, Hood AW, Brady CS. Nonlinear fast magnetoacoustic wave propagation in the neighborhood of a 22D magnetic X-point: oscillatory reconnection, astron. Astrophys 2008;493:227–40.
[8] Gruszecki M, Farahani SV, Nakariakov VM, Arber TD. Magnetoacoustic shock formation near a magnetic null point. Astron Astrophys 2011;531(A63):1–7.
[9] Nakariakov VM, Melnikov FF. Quasi-periodic pulsations in solar flares. Space-Sci Rev 2009;149:119–51.
[10] Varley E, Cumberbatch E. Non-linear theory of wave-front propagation. J Inst Math Appl 1965;1:101–12.
[11] Whitham GB. Linear and nonlinear waves. J. Wiley and Sons, NY; 1974.
[12] Jeffrey A. The formation of magnetoacoustic shocks. J Math Anal Appl 1965;11:139–50.
[13] Prasad P. Nonlinear hyperbolic waves in multi-dimensions. Chapman and Hall/CRC Press, Boca Raton, FL; 2001.
[14] Sharma VD. Quasilinear hyperbolic systems, compressible flows and waves. CRC Press, Boca Raton, FL; 2010.
[15] Majda AJ. One perspective on open problemas in multi-dimensional conservation laws. In: Glimm J, Majda A, editors. Multidimensional hyperbolic problemas and computations. Springer; 1991. p. 217–38.
[16] Rosales RR. An introduction to weakly nonlinear geometrical optics. In: Glimm J, Majda A, editors. Multidimensional hyperbolic problemas and computations. Springer; 1991. p. 281–310.
[17] Mikhalyaev BB. Discussion paper: the eigenoscillations of the solar active regions. Int J Geomagnet Aeronomy 2007;7:GI1003. doi:10.1029/2006GI000146.
[18] Cabannes H. Theoretical magnetofluid dynamics. Academic Press, NY; 1970.
[19] Núñez M. Some properties of the formation of fast magnetosonic shocks. Phys Lett A 2015;379:3108–13.